

Thermoelectric and Plasmonic Properties of Metal Nanoparticles Linked by Conductive Molecular Bridges

Aleksandr S. Fedorov,* Pavel O. Krasnov, Maxim A. Visotin, Felix N. Tomilin, and Sergey P. Polyutov*

Thermoelectric and plasmonic properties of systems comprising small golden nanoparticles (NPs) linked by narrow conductive polymer bridges are studied using the original hybrid quantum-classical model. The bridges are considered here to be either conjugated polyacetylene, polypyrrole, or polythiophene chain molecules terminated by thiol groups. The parameters required for the model are obtained using density functional theory and density functional tight-binding simulations. Charge-transfer plasmons in the considered dumbbell structures are found to possess frequency in the infrared region for all considered molecular linkers. The appearance of plasmon vibrations and the existence of charge flow through the conductive molecule, with manifestation of quantum properties, are confirmed using frequency-dependent polarizability calculations implemented in the coupled perturbed Kohn–Sham method. To study the thermoelectric properties of the 1D periodical systems, a universal equation for the Seebeck coefficient is derived. The phonon part of the thermal conductivity for the periodical $\text{–NP–S–C}_8\text{H}_8\text{–}$ system is calculated by the classical molecular dynamics. The thermoelectric figure of merit ZT is calculated by considering the electrical quantum conductivity of the systems in the ballistic regime. It is shown that for Au_{309} nanoparticles connected by polyacetylene, polypyrrole, or polythiophene chains at $T = 300$ K, the ZT value is $\{0.08; 0.45; 0.40\}$, respectively.

oscillations of free electrons and corresponding electromagnetic fields created by the charge motion inside the metal nanoparticles (NPs).^[1,2] Plasmonic materials are widely used in applications such as water splitting,^[3] photovoltaic cells,^[1,4–7] plasmon lasers,^[8] chemical synthesis,^[9] high-resolution imaging,^[10] and biomedical and telecom applications.^[11–14] LSP resonance is also actively utilized for nanoscale chemical and biological sensing.^[15–18] The sensor properties are conditioned here by the high sensitivity of the surface resonant frequency (SRF) to the permittivity of the surrounding chemical environment, which leads to the frequency shifting, for example, due to chemical adsorption.^[15–17,19]

The SRF strongly depends on the size and shape of NPs and the type of material between NPs.^[1,2,15–19] The reason for that is the strong dependence of the electromagnetic field strength, generated by LSPs, on distance and interaction between NPs. Therefore, there are a variety of different forms of plasmonic materials, such as

individual NPs of different shapes and materials^[20] and 2D lattices.^[11–13,21]

A presence of conductive material between two NPs leads to the emergence of a new mode, called the charge transfer plasmon (CTP), where the charge periodically moves between two NPs along a conductive bridge. For example, CTP was experimentally observed in a system consisting of two Au NPs linked by a thick gold bridge of radius ≈ 10 to 20 nm.^[16] This type of CTP can be described by classical Maxwell's electrodynamics as the quantum effects are not expected to be significant there due to large NPs and the bridge sizes. However, quantum effects of CTP have subsequently been investigated in systems consisting of two NPs separated by sub-nanometer interparticle gaps,^[22–24] where the coupling of NPs is conditioned by tunneling between them and by the screening effects. NP structures with conducting molecules 1,4-benzenedithiolate (BDT) and biphenyl-4,4'-dithiol (BPDT) that link cuboidal silver NPs^[25] and gold monolayers,^[26] respectively, were considered early. It was shown in both cases that the shifting of resonance energy of coupled plasmon and the creation of a screened coupled plasmon mode occur in the presence of some conducting linker. In the case of a biphenyl-1,4-thiol molecule, used instead of

1. Introduction


Localized surface plasmons (LSPs) have attracted remarkable attention in recent years due to their ability to enhance the local electromagnetic field in different optical processes that can be widely utilized in several applications. LSPs represent the

Prof. A. S. Fedorov, Dr. P. O. Krasnov, M. A. Visotin, Dr. F. N. Tomilin, Dr. S. P. Polyutov

Siberian Federal University
660041 Krasnoyarsk, Russia
E-mail: alex99@iph.krasn.ru; spolyutov@sfu-kras.ru

Prof. A. S. Fedorov, M. A. Visotin, Dr. F. N. Tomilin
Kirensky Institute of Physics
Federal Research Center KSC SB RAS
660036 Krasnoyarsk, Russia

Prof. A. S. Fedorov, Dr. F. N. Tomilin
Tomsk State University
634050 Tomsk, Russia

 The ORCID identification number(s) for the author(s) of this article can be found under <https://doi.org/10.1002/pssb.202000249>.

DOI: 10.1002/pssb.202000249

BDPT,^[26] which creates a chemical bond through only one sulfur atom linked to one of two Ag NPs (and, therefore, cannot be a conductor), and the use of an insulating 1,2-ethanedithiolate molecule instead of conducting BDT,^[25] the effects were not observed. However, so far, the CTP has not been extensively investigated for systems consisting of NPs linked by narrow conductive molecular bridges,^[27] where quantum effects are expected to be quite substantial. Aiming at this, we develop here a quantum-classical model for accurate description of such systems taking into account quantum effects and derive a general analytical expression for the shifted plasmonic frequencies. Finally, the thermoelectric properties of considered structures are estimated by the thermoelectric figure of merit ZT .

2. Modeling of CTPs in Dumbbell Structures

In our recent article,^[27] we considered a dumbbell structure consisting of two golden NPs linked by a narrow conductive molecular bridge and developed an original hybrid quantum-classical model to account for the quantum effects in CTP. The molecular bridge there has been modeled by a polyacetylene molecule C_nH_n terminated by two sulfur atoms, and the quantum effects in the bridge conductivity have been described utilizing first-principles density functional theory (DFT) simulations. As the bridge is thin and short in the model, it should be assumed that the movement of free carriers in the bridge has a ballistic character. Though the electron mobility in conductive polyacetylene, polypyrrole, and polythiophene chains is low, it could be increased by more than seven orders of magnitude upon doping with iodine or arsenic pentafluoride (AsF_5).^[28] Considering that in ordered materials, the average carrier mean free path is usually tens of nanometers even at room temperature, for conductive polymers, it reaches 330 Å at 1.8 K;^[18] it is natural to assume that in our case of a very short bridge, the carriers would move ballistically, wherein the gold NPs along the polymer chain edges play the role of dopants transforming the chain into a metallic state.

The conductivity in such a system and the transmission coefficient of the bridge can be calculated using the Keldysh nonequilibrium Green function (NEGF), which is widely used.^[29] Assuming that conduction band carriers pass from an NP into the bridge freely, the transmission coefficient, G , can be set as $G = (2e^2)/h \cdot M$, where M is several conductive channels in the bridge. Following the proposed model for dumbbell structures, one can note that two NPs have opposite electrostatic charges $Q(t)$ and opposite potentials. It results in charge transfer during plasmons' oscillations with a current $I(t) = \frac{dQ(t)}{dt}$ in the bridge. These structures can be considered as an LC oscillatory circuit, where the total capacitance C_{tot} is formed by the both NPs in the system having opposite charges, wherein the potential energy of the LC circuit is equal to

$$E_{pot} = Q^2 / (2C_{tot}) \quad (1)$$

where Q is the NP's charge. In ref. [27], it was confirmed with reasonable accuracy that the individual capacitance C of the considered gold NP is equal to the NP radius $C = R$, in full accordance with the classical theory of electrostatics. It also means that the entire additional charge of the NP is located

on its surface. For closely spaced NPs, the total capacitance is not equal to the sum of individual capacitance due to NPs' electrostatic interaction and polarization. It was shown in refs. [30,31] that the total potential energy of a couple of NPs with radius R and opposite charge Q is

$$E_{pot} = F(R, L) \frac{Q(t)^2}{2R + L} \quad (2)$$

where the fraction corresponds to the electrostatic interaction of the two opposite charges at a distance $2R + L$ between the NPs' centers. The correction function $F(R, L)$ considers the difference between the interaction of the two polarized spheres. In accordance with the articles cited earlier^[30,31] $F(R, L)$ decreases rapidly from 2.0 when two conducted spheres are touching, to 1.0, when $\frac{L}{2R} \rightarrow \infty$.

We argue that the analog of inductance in the dumbbell structure is formed by the current in the bridge. To confirm this, it is necessary to calculate the energy of conduction band carriers that create a current in the bridge. To calculate this current, we suppose that properties of the current in the NP–bridge–NP system are similar to the properties of the current in the periodical $[-NP\text{--}bridge\text{--}]$ system under the same electric bias. This assumption is based on the principle of locality of interactions. So, for simplicity, to find the current in the dumbbell structure, we calculate the band structure of a corresponding periodical system. Due to the periodic geometric structure of the bridge, we assume that the current in the bridge is formed by carriers in the conductive band (CB) having the parabolic dependence

$$E(k) = \frac{(\hbar k)^2}{2m^*} \quad (3)$$

where $m^* = \hbar^2 \left[\frac{d^2 E}{dk^2} \right]_{k=k_f}^{-1}$ is the electron (hole) effective mass in the bridge, wherein the current total kinetic energy E_{kin} of the conduction band electrons in the bridge can be written as a sum over electrons having different quasi-momentum

$$E_{kin} = \sum_{k,n} n_{k,n} \frac{\hbar^2 k_{k,n}^2}{2m^*} \quad (4)$$

where $n_{k,n}$ is the occupation number of electrons in the band n , which have quasi-momentum $k_{k,n}$.

Usually, the total time-dependent current in the bridge $I(t)$ can be calculated using the Landauer approach^[32]

$$I(t) = \frac{-e}{L} \sum_{k,n} n_{k,n} v_{k,n}^{eff} = \frac{2e^2}{h} M \frac{(\mu_1 - \mu_2)}{e} \quad (5)$$

$$v_{k,n}^{eff} = \frac{1}{\hbar} \frac{\partial E(k,n)}{\partial k} = \frac{\hbar k_{k,n}}{m^*} \quad (6)$$

where L is the length of the bridge, $v_{k,n}^{eff}$ is the effective electron velocity, M is the number of conductive channels in the bridge, and μ_1, μ_2 are the electrochemical potentials of both NPs having opposite charges. Therein the total current in the bridge is not zero because $n_{k,n}$ is different for the quasi-momentum of electrons moving in the bridge in opposite directions due to the difference of the NPs' electrochemical potentials. Using Equation (4) and (6) and supposing that our system forms a

degenerate metal, one can find the energy of the current in the bridge: $E_{\text{kin}} \sim I(t)^2$. This makes the aforementioned analogy between the NP–bridge–NP system and LC circuit reasonable.

But one should keep in mind that the current energy in the LC circuit relates to the energy of the magnetic field in space. In contrast, in the system considered here, it relates to the kinetic energy of carriers in the bridge. Unfortunately, the Landauer approach does not consider the acceleration of conduction band carriers in the electric field formed in the bridge by oppositely charged NPs. Subsequently we show a way to resolve this problem.

Considering the time derivative of the total energy of the system (potential (2) and kinetic (4) energies), which, neglecting the damping, should be equal to zero, dividing it by $I(t)$, and using formulas (1)–(6) of ref. [27], one can get a differential equation of the harmonic plasmon oscillations having the square of modified plasmonic frequency $\tilde{\omega}_{\text{pl}}^2$ in the dumbbell structure

$$\frac{d^2 Q(t)}{dt^2} = -\tilde{\omega}_{\text{pl}}^2 Q(t) \quad (7)$$

$$\tilde{\omega}_{\text{pl}}^2 = \left(\frac{1}{R} - \frac{F(R,L)}{2R+L} \right) \frac{2ne^2}{m^*L^2} \quad (8)$$

One can note here that $\tilde{\omega}_{\text{pl}}^2$ is similar to the square of conventional plasmonic frequency $\omega_{\text{pl}}^2 = 4\pi ne^2 / (m^* \Omega)$, where n denotes the number of conduction band electrons in the unit cell of volume Ω . To have qualitative estimation of the plasmonic frequency value, we neglect the second term in parentheses of Equation (8) and get the value

$$\tilde{\omega}_{\text{pl}}^2 \approx \frac{2ne^2}{m^*L^2R} = \frac{4\pi ne^2}{m^*\tilde{\Omega}} \quad (9)$$

where $\tilde{\Omega} = 2\pi RL^2$ —effective volume per n electrons.

Comparing $\tilde{\omega}_{\text{pl}}^2$ and ω_{pl}^2 , we can verify that the modified plasma frequency resides in the IR region. For example, for gold NPs having 147 atoms, radius $R \cong 7.41 \text{ \AA}$, and the bridge $[-\text{S}-\text{C}_8\text{H}_8-]$ with length $L \cong 14.3 \text{ \AA}$, the estimation of the modified plasma frequency gives $\tilde{\omega}_{\text{pl}} \approx 0.73 \text{ eV}$. One can see that in the proposed NP–bridge–NP systems, the plasmonic frequencies are expected to lie in the IR region and are sensitively changed with a change of the system dimensions.

2.1. Ab Initio Calculations of Dynamic Polarizability of the Au₅₅–polyacetylene–Au₅₅ Dumbbell Structure

To verify the validity of our model, we performed ab initio calculations of frequency-dependent complex polarizability for the test system, consisting of two gold NPs bridged by the conjugated polyacetylene molecule C₈H₈, terminated by sulfur atoms; see **Figure 1**. The calculations were performed within a combination of the atomic Gaussian-type orbital approach, as implemented in the CRYSTAL17 package.^[33] The GGA (generalized gradient approximation)-PBE (Perdew–Becke–Ernzerhof) approximation for the exchange–correlation functional^[34] was used for all calculations. The tolerance in the total energy difference between two subsequent iterations was set to 10^{-6} au. The gradients concerning atomic coordinates were evaluated analytically. An isolated

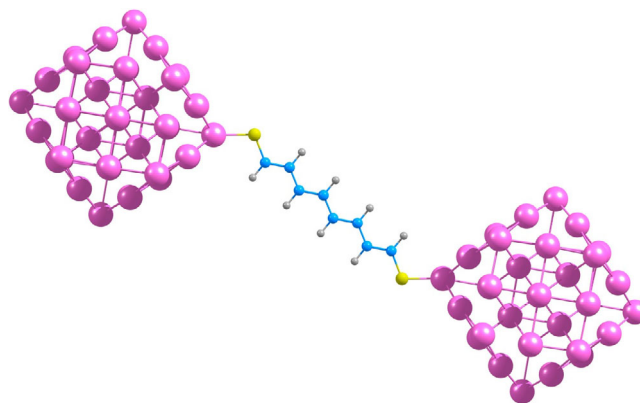


Figure 1. Geometry of Au₅₅–S–C₈H₈–Au₅₅ system.

gold NP of cuboctahedron shape having 55 atoms was optimized in O_h symmetry while Au₅₅–C₈H₈–Au₅₅ structure was optimized in C_{2h} symmetry (43 unique atoms). For calculations of frequency-dependent polarizability, the coupled perturbed Kohn–Sham (CPKS) method^[35] was used, wherein the damping factor (peak broadening) value related to the finite lifetime of excited states was chosen as 0.003 Hartree ($\approx 0.1 \text{ eV}$). The CPKS method is based on a perturbative treatment of the Schrödinger equation and its derivatives in the presence of an external electric field. The method allows us to consider the local field effects, i.e., change of the electrostatic and exchange–correlation potential under the electronic density variation in the external electric field. It allows us to calculate electronic density oscillations that correspond to CTPs in the NP–bridge–NP dimers. First, the dynamic polarizabilities of single Au₅₅ NPs and the dimer of these NPs without the bridge were calculated. One can see that in both cases, the positions of the peaks are almost the same. The amplitudes of the peaks are different due to the electrostatic interaction of NPs. The imaginary part of polarizability, which corresponds to the absorption cross-section of single NP, shows clear narrow resonances at 507, 544, and 721 nm (see inset in **Figure 2**). The IR region of the spectra with $\lambda > 750 \text{ nm}$ does not show any features for both cases.

We assume that the peak at 544 nm originates from an LSP, which agrees with experimental data on absorption of 5–20 nm monocrystalline gold NPs,^[36] where the plasmonic resonance is found at 520 nm. Therefore, we prove the CPKS method can reproduce an LSP. Next, the absorption of the polyacetylene conductive bridge alone (H–S–C₈H₈–H) was obtained; however, no clear resonances were found in vis–NIR spectra.

After that, the dynamic polarizability of the Au₅₅–S–C₈H₈–Au₅₅ dimer was calculated; the results for visible and IR regions are shown in **Figure 2** and **Figure 3**, respectively. The X-axis corresponds to the direction along the conductive bridge. Comparing the spectra of the dimer with those of a single particle, it can be seen that new resonant peaks emerge for the complex structure. In contrast, the heights and positions of the single-particle LSP peaks are significantly changed. The original plasmonic peak at 544 nm almost disappears for X and Y components, and in the Z component, the height is reduced to approximately four times. The 507 nm resonance is preserved in the X and Z directions, with a small redshift for the former, but completely absent for the Y-axis spectrum.

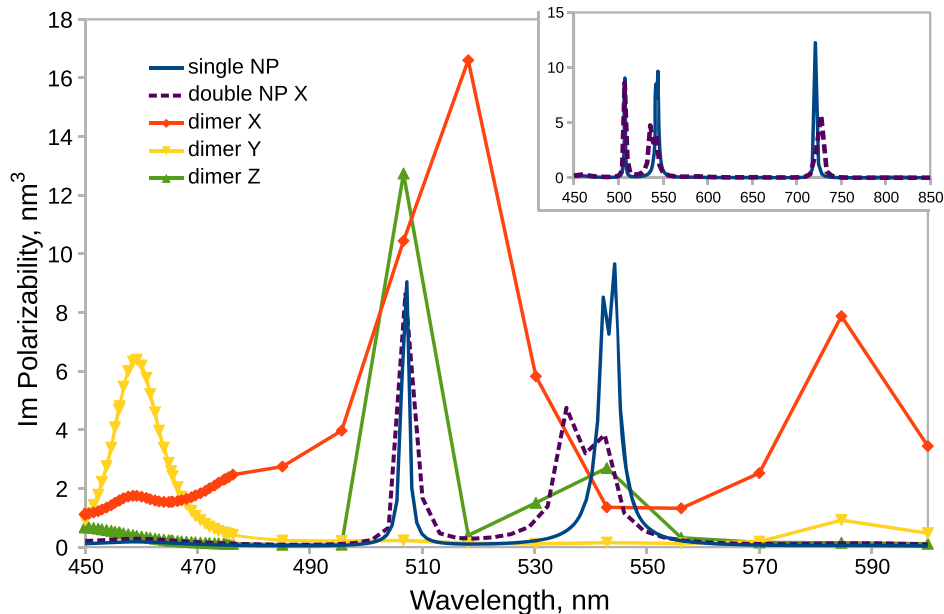


Figure 2. Imaginary part of dynamic polarizability in visible region of single Au_{55} NP, $\text{Au}_{55}\text{-S-C}_8\text{H}_8\text{-Au}_{55}$ dimer (three Cartesian components, dimer X, dimer Y, and dimer Z), and dimer of Au_{55} NPs without the polyacetylene bridge (along the dimer axis, double NP X).

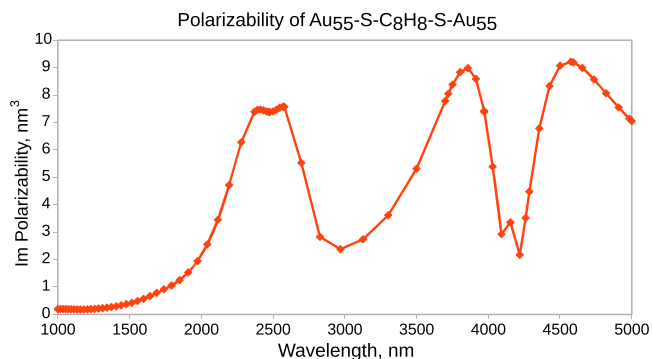


Figure 3. Imaginary part of dynamic polarizability of $\text{Au}_{55}\text{-S-C}_8\text{H}_8\text{-Au}_{55}$ dimer in the X direction along the conductive bridge, IR region.

The X component that is along the conductive bridge also shows a prominent feature at 565 nm.

The IR absorption spectra of the $\text{Au}_{55}\text{-S-C}_8\text{H}_8\text{-Au}_{55}$ dimer are characterized by three broad resonances in the X component, while the polarizability along the Y and Z directions is negligible ($< 0.03 \text{ nm}^3$). The magnitudes of the peaks at ≈ 2500 , ≈ 3850 , and $\approx 4600 \text{ nm}$ are comparable with those in the visible region of the spectra. While the imaginary part of the polarizabilities of single Au_{55} NPs and the polyacetylene conductive bridge do not exhibit any features at 1000–6000 nm range and their magnitudes are well below 0.002 nm^3 , these peaks arise due to the interaction of the $\text{-S-C}_8\text{H}_8\text{-}$ bridge with the NPs. The complex structure of the peak at 4000 nm has Fano lineshape and can be explained by the asymmetric attachment of the NPs to the polyacetylene chain. It leads to different interactions between the conduction electrons of the chain and the electrons of both NPs.

We have also applied Equation (9) of our model to calculate the plasmon frequency for this system. To do it, we choose the effective electron mass from ref. [27] as $m_{\text{eff}} = 0.455m_e$, the number of conductive electrons, which corresponds to the electrons in the conduction band, as $n = 2$, and the Au NP average radius as $R = 4.69 \text{ \AA}$. The calculated frequency $\tilde{\omega}_{\text{pl}} \approx 0.85 \text{ eV}$, which is equivalent to 1610 nm, lies on the border of large absorption with an agreement with Figure 3.

2.2. CTPs in Two NPs Connected by Polypyrrole or Polythiophene Bridge

It is well known now that, for example, polypyrrole and polythiophene are the organic polymer chains that have good electrical conductivity.^[37–39] They are more thermally and chemically resistant compared to the polyacetylene molecules studied as the linkers in our previous work,^[27] which motivates us to study them here.

Geometry optimization and calculations of band structures of two periodical chains, consisting of a Au_{309} NP and a fragment of polypyrrole (**Figure 4** and **5**) or polythiophene (**Figure 6** and **7**), were conducted by the self-consistent charge density functional

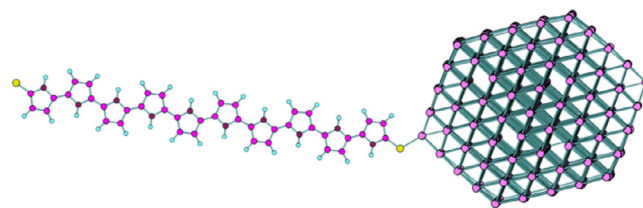


Figure 4. Optimized geometry of Au_{309} -polypyrrole unit cell (the length l is 62.878 \AA).

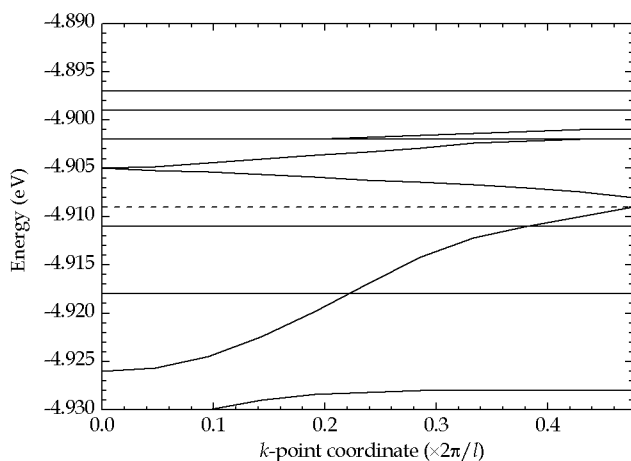


Figure 5. Band structure of Au_{309} -polypyrrole chain (dashed line is the Fermi level).

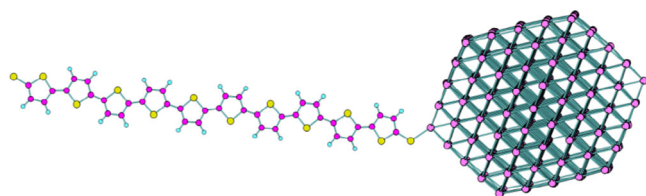


Figure 6. Optimized geometry of Au_{309} -polythiophene unit cell (the length l is 66.155 \AA).

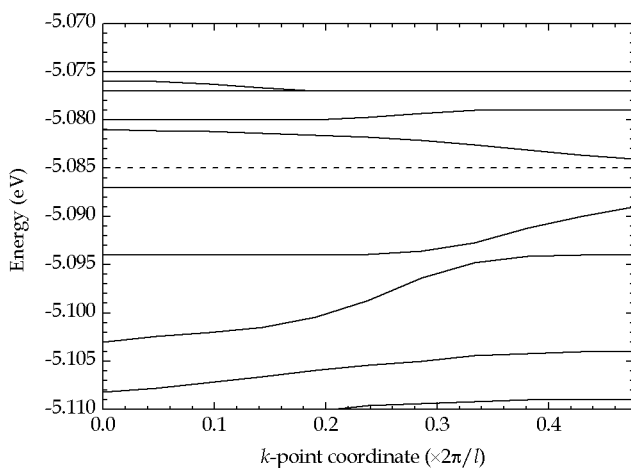


Figure 7. Band structure of Au_{309} -polythiophene chain (dashed line is the Fermi level).

tight-binding (SCC DFTB) method^[40] with use of the DFTB+ code (version 19.1)^[41] and a parameter set that is appropriate for the description of the interaction between the atoms in the series of carbon, nitrogen, oxygen, hydrogen, sulfur, and gold.^[40,42,43] Although the simulations were performed for periodic systems in the 3D space, the periodicity of these chains was considered along the x -direction. To prevent interaction of

the atoms in the unit cell with their replications along two other directions, the vacuum gap 50 \AA was applied and kept constant.

Both polypyrrole and polythiophene fragments consisted of ten heterocycles and had a length of 41.48 and 44.64 \AA , respectively. They were joined to Au NPs through the sulfur atoms. During the geometry optimization of both compounds, the k -point samplings of the first Brillouin zone (1BZ) were chosen as a $10 \times 1 \times 1$ mesh according to the Monkhorst-Pack scheme.^[44] At this, the relaxation was carried out by the conjugate limited-memory Broyden-Fletcher-Goldfarb-Shanno (LBFGS) algorithm until the forces acting on the atoms became less than 0.0001 au , and Fermi smearing was used at a finite temperature 600 K to enhance the convergence.

Band structure calculations were performed for optimized unit cells. The number of k -points was increased to 21 along the x -direction, while the finite temperature of Fermi smearing was decreased to 50 K .

Analyzing the band structures in Figure 5 and 7, it can be noted that in both cases, there are zones with zero dispersion. Obviously, they are formed by electronic states lying exclusively inside NPs, and therefore they can be excluded from our consideration of conductivity. Other zones have dispersion, which includes states inside the bridges. In the system with polypyrrole bridges, the zones of both types can intersect. It should be noted that in both cases, the zones are separated by a very small distance, so the electrons can jump between them due to thermal fluctuations.

By analyzing the average curvature of zones near E_{fermi} , the effective electron masses m_{eff} were calculated. They were equal to 0.502 , 0.446 , and $0.455 m_e$ for the systems with polypyrrole, polythiophene, and polyacetylene bridges, respectively.

After that, using the calculated m_{eff} and Equation (8) the $\tilde{\omega}_{\text{pl}}$ dependencies on the NP radius were constructed for the systems with these bridges; see Figure 8. It is shown there that the dependencies of $\tilde{\omega}_{\text{pl}}$ on R for the systems with polypyrrole and

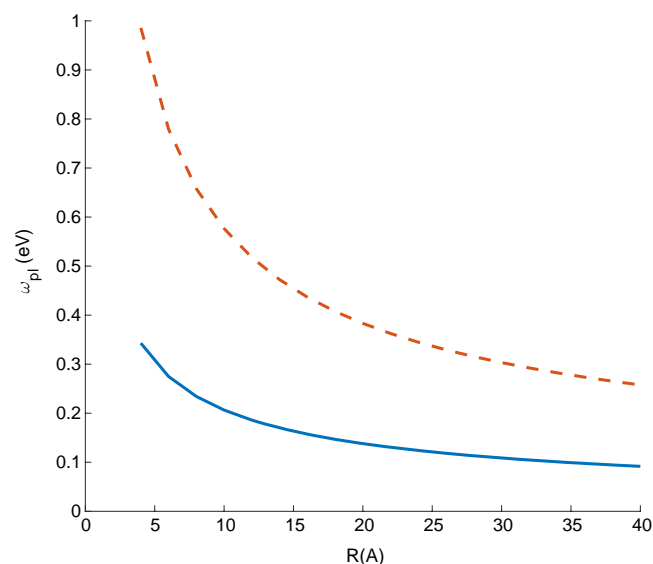


Figure 8. Dependence of $\tilde{\omega}_{\text{pl}}$ on NP radius, R . The solid line corresponds to the polypyrrole or polythiophene bridge and the dashed line to the $-\text{S}-\text{C}_8\text{H}_8-$ bridge.

polythiophene bridges are almost matched. The reason for that is both the almost identical lengths of the bridges and the effective electron mass in these systems. The dependence of $\tilde{\omega}_{\text{pl}}$ on R with the $[-\text{S}-\text{C}_8\text{H}_8-]$ bridge is significantly different due to the much shorter bridge length $L = 14.3 \text{ \AA}$. One can see in Equation (9) that the plasmonic frequency depends on the length L of the molecular bridge as L^{-2} , so the frequency rapidly decreases with increasing of L . The figure shows that in all cases the frequencies $\tilde{\omega}_{\text{pl}}$ lie in the IR region and quickly decrease with the NP size increasing.

3. Thermoelectric Properties of 1D Periodical Structures NP–Conductive Bridge

The field of thermoelectrics has made tremendous progress. It is currently growing steadily due to recent achievements and high global demand for cost-effective and environmentally friendly forms of energy conversion. The efficiency of thermoelectric materials is quantitatively determined by the thermoelectric figure of merit ZT , which is defined as $ZT = \frac{S^2 \sigma T}{\chi}$, where σ is the electrical conductivity, S is the thermoelectric power, χ is the total thermal conductivity, and T is the absolute temperature.

In the 1950s, alloys of Bi_2Te_3 were discovered to have $ZT \approx 1$ near room temperature, and they have played a dominant role in the field of thermoelectrics through today. Using simple calculations, it can be shown that at $ZT \approx 3 \div 4$ thermoelectric converters can successfully compete with plants based on heat engines (thermal power plants, etc.).

Therefore, obtaining materials with such ZT is the holy grail of researchers in this field. The successes of the last 10–15 years in this area have occurred mainly due to a new fundamental focus on nanostructured materials, which are considered very promising in this field. One of the possible methods here is the use of nanowires (NWs), since many theoretical studies predict a significant increase in ZT inside quantum wires due to additional electron confinement in directions perpendicular to the NW axis. Analysis of the electric and thermal transfer in different III–V and II–VI NWs shows that some systems with small effective electron mass (e.g., InSb) have the potential to achieve a high power factor and ZT values at acceptable experimentally achievable diameters ($D > 5 \text{ nm}$).^[45]

In ref. [46], the thermoelectric properties of NWs made of various lead compounds (PbS, PbSe, and PbTe) are investigated as a function of the length, diameter, and orientation on the base of Boltzmann transport equations. ZT values higher than 4 and 6 are predicted for 5 nm diameter PbSe/PbS and PbTe/PbSe superlattice NWs at 77 K, respectively. These ZT indicate that superlattice NWs are promising systems for thermoelectric applications.

In ref. [47], with first-principles calculations based on DFT theory, a very high thermoelectric figure of merit $ZT = 5$ at 800 K was predicted in an n-type Ba_2BiAu Heusler compound. Such a high efficiency arises from an intrinsically ultralow lattice thermal conductivity coupled with a very high power factor, which originates from a light, sixfold degenerate conduction-band pocket along the Γ – X direction. Weak acoustic phonon scattering and sixfold multiplicity combine to yield both high mobility and a high Seebeck coefficient.

Here we estimate ZT for $[-\text{NP-bridge}]$ periodical systems. The motivation for this is the ballistic transport of electrons in the conducting molecular bridges of the systems under consideration, affecting ZT . Also, the 1D nature of such systems and the excessively small width of the bridge can significantly change ZT .

Here we suppose that in the systems, the conduction band carriers have parabolic dependence of $E(k)$. Assuming this, we can suppose that the carriers' mobility, which is inversely proportional to the momentum-transfer collision frequency and effective mass, would not be changed during the movement inside the conduction band. This is because of the constant effective mass and mean travel time between collisions defined by the time of movement between two successive NPs.

So, the electrical current J through the system can be written as

$$J = \sigma E - \aleph \nabla T \quad (10)$$

where σ is an electrical conductivity and \aleph is a transport coefficient.^[48] The Seebeck coefficient S is defined as the voltage gradient produced in a sample by a given temperature gradient when the electrical current is zero: $S = \frac{\nabla \phi}{\nabla T} |_{J=0}$. It can be found as $S = \frac{\aleph}{\sigma}$.

To calculate it, we assume that there is a small temperature difference ΔT between two sequential NPs in the periodic structure. Because of this, the chemical potentials $\mu(T)$ of these NPs are shifted, which causes a current J to flow through the bridge. The current stops when the potential difference $\Delta \phi$ between the particles balances this temperature change of chemical potentials $\Delta \mu(T)$. Therefore, to find the potential difference $\Delta \phi$ and Seebeck coefficient S , correspondingly, one should calculate $\Delta \mu(T)$ at a given temperature change ΔT .

To calculate $\mu(T)$, one can use the following equation^[49]

$$\mu(T) = E_{\text{Fermi}} - \frac{\pi^2}{6} (k_b T)^2 \left[\frac{\partial}{\partial \epsilon} \ln(D(\epsilon)) \right]_{\epsilon=E_{\text{Fermi}}} \quad (11)$$

where $D(\epsilon)$ is the electronic density of states (DOS) that can be calculated by the well-known equality for 1D systems

$$D(\epsilon) = \frac{\sqrt{m^*}}{\sqrt{2\pi\hbar}\sqrt{e}} \quad (12)$$

Here we again suppose that in the periodical $[-\text{NP-bridge}]$ systems, the conduction band carriers have parabolic dependence (Equation (3)). To eliminate the ambiguity, we will further measure the E_{Fermi} from the bottom of the conduction band. Using Equation (11, 12 and 3), one can easily get

$$\mu(T) = E_{\text{Fermi}} + \frac{\pi^2}{12} \frac{(k_b T)^2}{E_{\text{Fermi}}} \quad (13)$$

$$S = \frac{\nabla \phi}{\nabla T} = \frac{\pi^2}{6} \frac{k_b^2 T}{e E_{\text{Fermi}}} \quad (14)$$

For the periodical systems of NPs connected by polyacetylene, polypyrrole, and polythiophene chain molecules (see Figure 4 and 6) and assuming that the temperature is $T = 300 \text{ K}$,

one can calculate $S = \{90; 212; 201\} \mu\text{V K}^{-1}$ for the three bridges, respectively.

The knowledge of thermopower S gives the possibility to calculate the thermoelectric figure of merit

$$ZT = \frac{S^2 \sigma T}{\chi_{\text{el}} + \chi_{\text{vibr}}} \quad (15)$$

where χ_{el} and χ_{vibr} are the electronic and phononic contributions to the thermal conductivity, respectively. χ_{el} can be calculated using the Wiedemann–Franz law

$$\frac{\chi_{\text{el}}}{\sigma} = L_0 T, \text{ where } L_0 = \frac{\pi^2}{3} \left(\frac{k_{\text{B}}}{e}\right)^2 = 2.47 \times 10^{-8} \text{ W ohm K}^{-2} \quad (16)$$

In ref. [27] we show that the conductance G of a similar system $[\text{NP-S-C}_{16}\text{H}_{16}\text{-Au}_{55}\text{-S}]$ is

$$G \simeq (2e^2)/h = (12.9 \times 10^3 \text{ ohm})^{-1} \quad (17)$$

so we suppose the our system conductance is similar.

Assuming the ballistic motion of carriers in the 1D systems, the conductivity of the system has a quantized character. It does not depend on the properties (effective mass) of carriers. It is determined only by the number of conductive modes and properties of the interface region between the NP and the conducting bridge. For the narrow conductive bridges under consideration, one can assume that the number of these modes is equal to 1, except for spin degeneracy. All other modes will be suppressed due to the narrowness of the conducting channel and the Coulomb blockade effect, which can be expected for such systems.^[50]

Using $\sigma = G \frac{L}{S}$, where L and S are longitudinal size and transverse sections of the unit cell and applying Equation (16) one can get $\chi_{\text{el}} = 0.25 \text{ W m}^{-1} \text{ K}^{-1}$.

Let us note that the calculation of the thermal conductivity associated with atomic vibrations χ_{vibr} is a rather difficult task that can be solved using molecular dynamics (MD) simulations. To do it, the LAMMPS (Large-scale Atomic/Molecular Massively Parallel Simulator) software^[51,52] was used. The interactions within the polyacetylene chain were calculated using empirical potentials of the REBO type,^[53] while gold atoms' interactions were calculated using the embedded atom model (EAM) method.^[54]

The phonon thermal conductivity $\chi_{\text{vibr}} = 0.77 \text{ W m}^{-1} \text{ K}^{-1}$ was calculated by the Kubo–Green method at temperature $T = 300 \text{ K}$ for a periodical chain of Au_{309} NPs connected by conjugated polyacetylene molecule C_8H_8 , terminated by sulfur atoms.

So, one can see the phonon contribution prevails over the electronic one in the total thermal conductivity.

Assuming the electrical conductivity of the aforementioned periodical systems including polyacetylene, polypyrrole, and polythiophene chains is similar to (16) and the thermal conductivity is akin also, one can find the $ZT \lesssim \{0.08; 0.45; 0.40\}$ at temperature $T = 300 \text{ K}$ for each of the linkers, respectively.

4. Conclusion

CTPs and thermoelectric properties of gold NPs bridged by conductive polyacetylene, polypyrrole, and polythiophene molecules were studied. To describe CTPs of the dumbbell systems consisting of two metal NPs connected by a conductive bridge, an original quantum-classical model was used. The model utilizes the analogy with an LC oscillatory circuit and is based on a description of the time-dependent ballistic current through the bridge. The model takes into account quantum effects. Based on this model, we have derived a general analytical expression for the plasmon frequency for the dumbbell systems and have shown that its frequency lies in the IR region. It is shown that the frequencies are highly dependent on the system size and conductivity of the bridge.

Thermoelectric properties of periodic 1D systems consisting of NPs connected by polyacetylene, polypyrrole, or polythiophene polymer bridges are considered. In the beginning, we have derived the universal equation for calculation of the Seebeck coefficient that, then, has been used for calculation of thermal conductivity of the NP–polyacetylene system by classical molecular dynamics. Here we assume that the thermal conductivities of the aforementioned systems are similar and take into account that the electrical quantum conductivity of the systems in the ballistic regime is roughly equal to one quantum ($2e^2/h$). Finally, using the state that thermal conductivity is, in turn, proportional to electrical quantum conductivity, we have calculated the thermoelectric figure of merit ZT . It is shown that for Au_{309} NPs connected by polyacetylene, polypyrrole, or polythiophene chains at $T = 300 \text{ K}$, exhibit $ZT \sim \{0.08; 0.45; 0.40\}$, respectively.

Acknowledgements

This study was supported by the Russian Science Foundation, project no. 16-13-00060 (thermoelectric properties), and by the Ministry of Science and High Education of the Russian Federation, project no. FSRZ-2020-0008 (plasmonic properties).

Conflict of Interest

The authors declare no conflict of interest.

Keywords

charge transfer plasmons, density functional theory, nanoparticles, thermoelectric properties

Received: April 30, 2020
Revised: September 17, 2020
Published online:

- [1] A. Uddin, X. Yang, *J. Nanosci. Nanotechnol.* **2014**, *14*, 1099.
- [2] J. Liu, H. He, D. Xiao, S. Yin, W. Ji, S. Jiang, D. Luo, B. Wang, Y. Liu, *Materials* **2018**, *11*, 1833.
- [3] M. Valenti, M. P. Jonsson, G. Biskos, A. Schmidt-Ott, W. A. Smith, *J. Mater. Chem. A* **2016**, *4*, 17891.
- [4] F. Parveen, B. Sannakki, M. V. Mandke, H. M. Pathan, *Sol. Energy Mater. Sol. Cells* **2016**, *144*, 371.

- [5] S. Gwo, H.-Y. Chen, M.-H. Lin, L. Sun, X. Li, *Chem. Soc. Rev.* **2016**, *45*, 5672.
- [6] K. Ueno, T. Oshikiri, Q. Sun, X. Shi, H. Misawa, *Chem. Rev.* **2018**, *118*, 2955.
- [7] N. Venugopal, V. Gerasimov, A. Ershov, S. Karpov, S. Polyutov, *Opt. Mater.* **2017**, *72*, 397.
- [8] C. Deeb, J.-L. Pelouard, *Phys. Chem. Chem. Phys.* **2017**, *19*, 29731.
- [9] S. Linic, U. Aslam, C. Boerigter, M. Morabito, *Nat. Mater.* **2015**, *14*, 567.
- [10] K. A. Willets, A. J. Wilson, V. Sundaresan, P. B. Joshi, *Chem. Rev.* **2017**, *117*, 7538.
- [11] A. D. Utyushev, I. L. Isaev, V. S. Gerasimov, A. E. Ershov, V. I. Zakomirnyi, I. L. Rasskazov, S. P. Polyutov, H. Ågren, S. V. Karpov, *Opt. Express* **2020**, *28*, 1426.
- [12] V. Gerasimov, A. Ershov, R. Bikbaev, I. Rasskazov, I. Timofeev, S. Polyutov, S. Karpov, *J. Quant. Spectrosc. Radiat. Transf.* **2019**, *224*, 303.
- [13] V. I. Zakomirnyi, I. L. Rasskazov, V. S. Gerasimov, A. E. Ershov, S. P. Polyutov, S. V. Karpov, *Appl. Phys. Lett.* **2017**, *111*, 123107.
- [14] A. E. Ershov, V. S. Gerasimov, R. G. Bikbaev, S. P. Polyutov, S. V. Karpov, *J. Quant. Spectrosc. Radiat. Transf.* **2020**, *248*, 106961.
- [15] L. Guo, J. A. Jackman, H.-H. Yang, P. Chen, N.-J. Cho, D.-H. Kim, *Nano Today* **2015**, *10*, 213.
- [16] A. N. Koya, J. Lin, *Appl. Phys. Rev.* **2017**, *4*, 021104.
- [17] N. Elahi, M. Kamali, M. H. Baghersad, *Talanta* **2018**, *184*, 537.
- [18] Z. Farka, T. Juřík, D. Kovář, L. Trnková, P. Skládal, *Chem. Rev.* **2017**, *117*, 9973.
- [19] J. Olson, S. Dominguez-Medina, A. Hoggard, L.-Y. Wang, W.-S. Chang, S. Link, *Chem. Soc. Rev.* **2015**, *44*, 40.
- [20] V. I. Zakomirnyi, I. L. Rasskazov, S. V. Karpov, S. P. Polyutov, *J. Quant. Spectrosc. Radiat. Transf.* **2017**, *187*, 54.
- [21] S. G. Moiseev, I. A. Glukhov, Y. S. Dadoenkova, F. F. L. Bentivegna, *J. Opt. Soc. Am. B* **2019**, *36*, 1645.
- [22] R. Esteban, A. G. Borisov, P. Nordlander, J. Aizpurua, *Nat. Commun.* **2012**, *3*, 825.
- [23] R. Esteban, A. Zugarramurdi, P. Zhang, P. Nordlander, F. J. García-Vidal, A. G. Borisov, J. Aizpurua, *Faraday Discuss.* **2015**, *178*, 151.
- [24] W. Zhu, R. Esteban, A. G. Borisov, J. J. Baumberg, P. Nordlander, H. J. Lezec, J. Aizpurua, K. B. Crozier, *Nat. Commun.* **2016**, *7*, 11495.
- [25] S. F. Tan, L. Wu, J. K. W. Yang, P. Bai, M. Bosman, C. A. Nijhuis, *Science* **2014**, *343*, 1496.
- [26] F. Benz, C. Tserkezis, L. O. Herrmann, B. de Nijs, A. Sanders, D. O. Sigle, L. Pukenas, S. D. Evans, J. Aizpurua, J. J. Baumberg, *Nano Lett.* **2015**, *15*, 669.
- [27] A. Fedorov, P. Krasnov, M. Visotin, F. Tomilin, S. Polyutov, H. Ågren, *J. Chem. Phys.* **2019**, *151*, 244155.
- [28] A. B. Kaiser, *Rep. Prog. Phys.* **2001**, *64*, 1.
- [29] G. Stefanucci, R. van Leeuwen, *Nonequilibrium Many-Body Theory of Quantum Systems*, Cambridge University Press, Cambridge **2013**.
- [30] W. R. Smythe, *Static and Dynamic Electricity*, 2nd edition, McGraw-Hill Book Company, Inc., New York, NY **1950**, p. 616.
- [31] V. A. Saranin, *Physics-Uspekhi* **1999**, *42*, 385.
- [32] R. Landauer, *Philos. Mag.* **1970**, *21*, 863.
- [33] R. Dovesi, A. Erba, R. Orlando, C. M. Zicovich-Wilson, B. Civalleri, L. Maschio, M. Rérat, S. Casassa, J. Baima, S. Salustro, B. Kirtman, *WIREs Comput. Mol. Sci.* **2018**, *8*, e1360.
- [34] J. P. Perdew, K. Burke, M. Ernzerhof, *Phys. Rev. Lett.* **1996**, *77*, 3865.
- [35] M. Ferrero, M. Rérat, B. Kirtman, R. Dovesi, *J. Chem. Phys.* **2008**, *129*, 244110.
- [36] C. Zhou, J. Yu, Y. Qin, J. Zheng, *Nanoscale* **2012**, *4*, 4228.
- [37] W.-F. Su, *Principles of Polymer Design and Synthesis*, Lecture Notes in Chemistry, Vol. 82, Springer, Berlin **2013**, pp. 185–218.
- [38] T. V. Vernitskaya, O. N. Efimov, *Uspekhi Khimii* **1997**, *66*, 502.
- [39] A. G. MacDiarmid, *Angew. Chem.* **2001**, *40*, 2581.
- [40] M. Elstner, D. Porezag, G. Jungnickel, J. Elsner, M. Haugk, T. Frauenheim, S. Suhai, G. Seifert, *Phys. Rev. B* **1998**, *58*, 7260.
- [41] B. Aradi, B. Hourahine, T. Frauenheim, *J. Phys. Chem. A* **2007**, *111*, 5678.
- [42] T. Niehaus, M. Elstner, T. Frauenheim, S. Suhai, *J. Mol. Struct.: THEOCHEM* **2001**, *541*, 185.
- [43] A. Fihey, C. Hettich, J. Touzeau, F. Maurel, A. Perrier, C. Köhler, B. Aradi, T. Frauenheim, *J. Comput. Chem.* **2015**, *36*, 2075.
- [44] H. J. Monkhorst, J. D. Pack, *Phys. Rev. B* **1976**, *13*, 5188.
- [45] D. A. Broido, N. Mingo, *Mater. Phys.* **2006**, *74*, 195325.
- [46] Y. M. Lin, S. Dresselhaus, *Mater. Phys.* **2003**, *68*, 075304.
- [47] J. Park, Y. Xia, V. Ozolinš, *Phys. Rev. Appl.* **2019**, *11*, 014058.
- [48] J. Scheidemantel, C. Ambrosch-Draxl, T. Thonhauser, V. Badding, O. Sofo, *Mater. Phys.* **2003**, *68*, 125210.
- [49] J. Ziman, *Principles of the Theory of Solids*, Cambridge University Press, Cambridge **1979**.
- [50] S. Datta, *Electronic Transport in Mesoscopic Systems*, Cambridge University Press, Cambridge **1995**.
- [51] LAMMPS Molecular Dynamics Simulator, <https://lammmps.sandia.gov> (accessed: August 2020).
- [52] S. Plimpton, *J. Comput. Phys.* **1995**, *117*, 1.
- [53] S. J. Stuart, A. B. Tutein, J. A. Harrison, *J. Chem. Phys.* **2000**, *112*, 6472.
- [54] M. S. Daw, M. I. Baskes, *Phys. Rev. B* **1984**, *29*, 6443.